Heliyon 10 (2024) e29560

Contents lists available at ScienceDirect

Heliyon

journal homepage: www.cell.com/heliyon

Research article

Virtual screening, MMGBSA, and molecular dynamics approaches for identification of natural products from South African biodiversity as potential *Onchocerca volvulus* pi-class glutathione S-transferase inhibitors

Mbah Bake Maraf [a,b,**], Bel Youssouf G. Mountessou [b], Tsahnang Fofack Hans Merlin [c,d], Pouyewo Ariane [a,b], Joëlle Nadia Nouping Fekoua [a,b], Takoua Bella Jean Yves [b], Tchuifon Tchuifon Donald Raoul [e], Auguste Abouem A Zintchem [b], Gouet Bebga [b], Ndassa Ibrahim Mbouombouo [b,f,*], Ponnadurai Ramasami [g,h,***]

[a] *Physical and Theoretical Chemistry Unit, Laboratory of Applied Physical and Analytical Chemistry, Faculty of Science, University of Yaoundé I, P. O. BOX 812, Yaoundé, Cameroon*
[b] *Computational Chemistry Laboratory, Department of Chemistry, Higher Teacher Training College, University of Yaoundé I, P. O. Box 47, Yaoundé, Cameroon*
[c] *Laboratoire Optique et Applications, Centre de Physique Atomique Moléculaire et Optique Quantique, Faculté des Sciences, Université de Douala, B. P. 8580, Douala, Cameroon*
[d] *Analytical, Structural and Materials Chemistry Laboratory, Department of Chemistry, Faculty of Science, University of Douala, B.P. 24157, Douala, Cameroon*
[e] *Department of Process Engineering, Laboratory of Energy, Materials, Modeling and Method, National Higher Polytechnic School of Douala, University of Douala, P.O. Box 2701 Douala, Cameroon, Douala*
[f] *Department of Applied Chemistry, Faculty of Science, University of Ebolowa, P.O. Box 118, Ebolowa, Cameroon*
[g] *Computational Chemistry Group, Department of Chemistry, Faculty of Science, University of Mauritius, Réduit, 80837, Mauritius*
[h] *Centre for Natural Product Research, Department of Chemical Sciences, University of Johannesburg, Doornfontein, 2028, South Africa*

ARTICLE INFO

Keywords:
Onchocerca volvulus pi-class glutathione S-Transferase
South African natural products
Virtual screening
MMGBSA
Molecular dynamics

ABSTRACT

We investigated 1012 molecules from natural products previously isolated from the South African biodiversity (SANCDB, https://sancdb.rubi.ru.ac.za/), for putative inhibition of *Onchocerca volvulus* pi-class glutathione *S*-transferase (Ov-GST2) by virtual screening, MMGBSA, and molecular dynamics approaches. ADMET, docking, and MMGBSA shortlisted 12 selected homoisoflavanones-type hit molecules, among which two namely SANC00569, and SANC00689 displayed high binding affinities of −46.09 and −46.26 kcal mol−1, respectively towards π-class Ov-GST2, respectively. The molecular dynamics results of SANC00569 showed the presence of intermolecular H-bonding, hydrophobic interactions between the ligand and key amino acids of

* Corresponding author. Computational Chemistry Laboratory, Department of Chemistry, Higher Teacher Training College, University of Yaoundé I, P. O. Box 47, Yaoundé, Cameroon.
** Corresponding author. Physical and Theoretical Chemistry Unit, Laboratory of Applied Physical and Analytical Chemistry, Faculty of Science, University of Yaoundé I, P.O. BOX 812, Yaoundé, Cameroon.
*** Corresponding author. Computational Chemistry Group, Department of Chemistry, Faculty of Science, University of Mauritius, Réduit, 80837, Mauritius.
E-mail addresses: mbahbakemaraf@yahoo.com (M.B. Maraf), indassa@yahoo.fr (N.I. Mbouombouo), p.ramasami@uom.ac.mu (P. Ramasami).

https://doi.org/10.1016/j.heliyon.2024.e29560
Received 15 December 2023; Received in revised form 8 April 2024; Accepted 10 April 2024
Available online 18 April 2024
2405-8440/© 2024 Published by Elsevier Ltd. This is an open access article under the CC BY-NC-ND license (http://creativecommons.org/licenses/by-nc-nd/4.0/).

Ov-GST2, throughout the simulation period. This hit molecule had a stable binding pose and occupied the binding pockets throughout the 200 ns simulation. To the best of our knowledge, there is no report of any alleged anti–onchocerciasis activity referring to homoisoflavanones or flavonoids. Nevertheless, homoisoflavanones, which are a subclass of flavonoids, exhibit a plethora of biological activities. All these results led to the conclusion that SANC00569 is the most hypothetical Ov-GST2, which could lead the development of new drugs against *Onchocerca volvulus* pi-class glutathione *S*-transferase. Further validation of these findings through in vitro and in vivo studies is required.

1. Introduction

Onchocerciasis, also known as river blindness, is a neglected parasitic disease caused by a worm called *Onchocerca volvulus* that is transmitted bites from infected simulium (black flies). The simuliums carry the immature form of the worm and transmit it from human to human. In the human body, the adult female worm produces thousands of worms (microfilariae) per day. These microfilariae spread throughout the body by moving under the skin causing damage such as skin rashes, lesions, itching, and depigmentation. They are highly toxic to the skin and eyes, causing terrible itching of the skin and damage of the eyes that lead, after multiple years of exposure, to irreversible blindness [1].

Over the years, microfilariae have been the target of treatment with ivermectin® (IVM), the most widely administered drug for treating onchocerciasis due to its good tolerance level and high efficacy. Onchocerciasis remains a public health problem in endemic communities despite advances made by ivermectin® treatment in reducing the burden of the disease. Unfortunately, ivermectin® is not used on humans co-infected with loiasis owing to potentially serious adverse effects [2]. Another treatment approach is doxycycline®, an antibiotic targeting the bacterial organisms *Wolbachia* which co-habit with filarial nematodes in a somewhat endosymbiotic fashion. However, doxycycline® is not compelling enough for mass drug administration due to its long treatment period of 4–6 weeks and contraindications in children and pregnancy [3]. A useful class of compounds with a broad spectrum of anti-helminthic activities are the benzimidazoles, amino-acetonitriles derivatives which kill both larvae and adult nematodes with generally low human toxicity except that they are associated with teratogenicity and embryotoxicity. In addition, flubendazole® (FBZ) which is an approved drug for treating gastrointestinal nematodes in humans, has also been reported as an active agent against organisms causing onchocerciasis [4]. Closantel®, a well-known veterinary anti-helmintic agent, was identified to have new activity: it is a potent and specific competitive inhibitor of the chitinase from *O. volvulus* (OvCHT1) [5].

The current treatments for onchocerciasis have limitations, including safety concerns, long treatment periods, and contraindications in specific populations. Therefore, there is a critical need for new, more effective, and safer treatment options to combat this parasitic disease and improve patient outcomes. In the search for new strategies of managing onchocerciasis, researchers have been investigating molecules which might prevent infections from *Onchocerca* spp. For instance, Ugbe et *al.,* studied the effect of prostaglandin D synthase (PDB: 2HNL) and π-class glutathione *S*-transferase (PDB: 1TU7), both of which are the enzyme class transferase and function similarly on *O. volvulus*. They showed that the Molecular Dynamics simulation performed on the docked complexes of twenty molecules and flubendazole® confirmed the rigidity and stability of their interactions. Moreover, they came out with the conclusion that twenty selected molecules could be considered as superior drug candidates for the treatment of onchocerciasis [4]. Wu et *al.* [6], found that chitinases expressed by infective stages of the filarial nematodes may play a role in ecdysis during post-infective development. They also found that DNA vaccination with the chitinase gene Ov-CHT1, a L3 specific chitinase from acanthocheilonema viteae, induced protection against the infective L3 of O. volvulus in mice.

Glutathione-*S*-transferases (GSTs) are a family of Phase II detoxification enzymes that catalyzes the conjugation of glutathione (GSH) to a wide variety of endogenous and exogenous electrophilic compounds. GSTs are divided into two distinct super-family members: the membrane-bound microsomal and cytosolic family members. Microsomal GSTs are structurally distinct from the cytosolic members in that they homo- and heterotrimerize rather than dimerize to form a single active site. Microsomal GSTs play a key role in the endogenous metabolism of leukotrienes and prostaglandins. Human cytosolic GSTs are highly polymorphic and can be divided into six classes: α, μ, ω, π, θ, and ζ. The π and μ classes of GSTs play a regulatory role in the nitrogen-activated protein (MAP) kinase pathway that participates in cellular survival and death signals via protein: protein interactions with c-Jun N-terminal kinase 1 (JNK1) and ASK1 (apoptosis signal-regulating kinase) [7].

It is noteworthy that Computer-Aided Drug Design (CADD) is crucial in drug discovery. It saves time and cost, and tends to be highly effective for evaluating a sizeable virtual database of chemical compounds. For researchers working on CADD, natural products represent an untapped and rich reservoir for the discovery of efficient drugs or lead compounds. Natural products have shown great potentials in treating infectious diseases in humans [8] and they have been suggested to be a good alternative to ant-filarial medicines because they are cheap, readily available, have negligible side effects and their compliance rate may be high since they are indigenous medicines [9]. The successful development of new drugs with improved efficacy and safety profiles can have a significant impact on public health in endemic communities. These drugs could lead to better disease management, reduced transmission rates, and improved quality of life for individuals suffering from onchocerciasis. Additionally, more effective treatments can contribute to the overall control and elimination efforts of onchocerciasis, ultimately benefiting the community by reducing the burden of this neglected tropical disease.

In this study, virtual screening, Molecular Mechanics-Generalized Born Surface Area (MMGBSA), and Molecular Dynamics (MD)

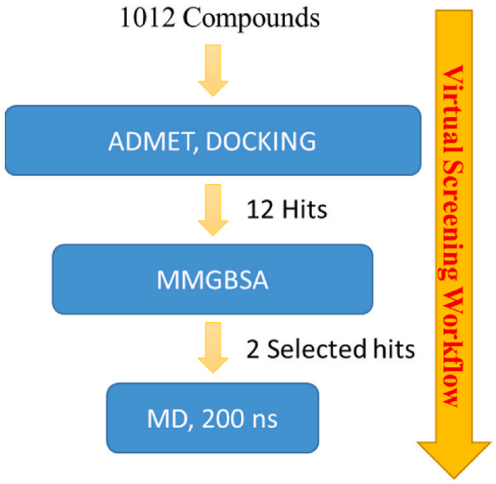

Fig. 1. Workflow of the virtual screening approach for the identification of potential O. *volvulus* pi-class glutathione *S*-transferase inhibitors.

simulation were conducted to find suitable drug candidates among some 1012 natural products isolated from species of the South African biodiversity (SANCDB), for the treatment of onchocerciasis. The use of the South African natural compound database (SANCDB) can be justified for several reasons. Firstly, the database likely contains unique compounds specific to the region's biodiversity, offering a diverse and novel chemical space for exploration. Secondly, utilizing local natural products enhances the potential for discovering bio active compounds with pharmacological relevance. Thirdly, studying compounds from South African biodiversity may lead to the identification of new drug leads with distinct mechanisms of action. Additionally, focusing on indigenous sources aligns with the principles of sustainable drug discovery and supports local scientific research initiatives. Overall, leveraging the South African natural compound database provides an opportunity to uncover valuable compounds for potential therapeutic applications.

2. Materials and methods

2.1. Target protein structure and ligand preparation

The crystal structure of the *O. volvulus* pi-class glutathione *S*-transferase, Ov-GST2 (PDB code: 1tu8) was retrieved from the Protein Data Bank (www.rcsb.org). Errors in the target's crystal structure were fixed using the protein preparation wizard in Schrödinger suite 2021-1-3 [10]. This was done by assigning bond ordering and adding missing hydrogen atoms with energetic optimization performed in the last step of refining the preparation by OPLS3 force field (a force field providing broad coverage of drug-like small molecules and proteins) [11] and root mean square deviation (RMSD) of the heavy atoms set to 0.3 Å. By selecting the crystalline ligand at the target's active site, the receptor grid generating tool automatically created the x, y, and z coordinates to generate the glide grid file ($x = 11$, $y = 13$, $z = 14$). The sdf file of the studied molecules were retrieved from the South African natural compounds database (SANCDB, https://sancdb.rubi.ru.ac.za/) and imported into the workspace of the maestro 11 [12]. The LigPrep module [13] in maestro's Schrödinger suite was used to prepare these molecules. At a physiological pH of 7.2 ± 0.2, the potential ionization states for each ligand structure were computed. The ligands were minimized using an OPLS3 force field, and all other settings were left at their default settings.

2.2. ADMET, docking & MMGBSA

QikProp was used to test the 1012 molecules for toxicity and drug-likeness [14]. The Lipinski rule of five (RO5), GI absorption, inhibition of CYP450 isoenzymes, hepatotoxicity, eye irritation and corrosion, biodegradation, and other factors were used to filter the compounds. The selected compounds from the ADMET screening were docked using the high throughput virtual screening (HTVS), standard precision (SP) and the extra precision (XP) glide docking filtering methods, respectively. Afterwards, the MMGBSA method in Prime was used for rescoring the docked pose of the 12 selected hit compounds from extra precision (XP) [15]. These poses were taken as inputs for the energy minimization of the protein-ligand complexes ($E_{complex}$), the free protein ($E_{protein}$), and the free ligands (E_{ligand}). The binding free energy ΔG_{bind} was simply evaluated as[16]:

$$\Delta G_{bind} = E_{\_complex\ (minimized)} - E_{\_ligand\ (minimized)} - E_{\_receptor\ (minimized)} \quad (1)$$

The docking scores, binding affinities, Glide Gscores, Glide energies, and Glide emodels were then utilized to quantify the docking calculation's outcomes.

Table 1
QikProp pharmacokinetic and toxicity predictions of selected ligands.

Ligand	SASA	FOSA	FISA	PISA	WPSA/RO3/5	volume	donorHB	accptHB	HOA	PHO	PSA	QplogS	CIQPlogS	QPlogHERG	QPPCaco	QPlogBB
SANC00569	594.88	252.73	210.44	131.72	0	1046.53	3	6.25	2	72.61	130.12	−3.53	−4.81	−4.78	100.08	−1.92
SANC00101	514.19	64.21	238.02	211.96	0	873.27	5	5.45	2	60.94	115.5	−2.66	−3.47	−4.82	54.8	−1.89
SANC00689	528.2	129.85	126.14	272.21	0	913.35	1	3.75	3	93.73	84.46	−3.78	−4.73	−5.07	630.58	−0.87
SANC00317	0	0	0	0	5	0	−2	304.26	−4.93	23.02	−5.4	6.45	0.03	0.02	0.85	27.83
SANC00520	517.5	0	285.85	231.65	0	866.48	4	5.25	2	52.2	142.68	−2.88	−4.04	−5.07	19.29	−2.38
SANC00335	496.05	44.29	183.83	267.93	0	836.4	2	4	3	77.52	98.61	−3.37	−3.93	−4.99	178.93	−1.25
SANC00263	546.78	92.67	239.14	214.97	0	923.14	3	5.25	3	64.88	128.56	−3.47	−4.4	−5.17	53.47	−2.01
SANC00106	0	0	0	0	3/0/0	0	−2	272.26	−5.12	211.87	−3.45	4.95	0.02	0.01	0.86	28.08
SANC00643	501.18	48.9	198.44	253.83	0	840.08	2	4	3	74.46	100.3	−3.46	−3.93	−5.02	130.04	−1.41
SANC00105	506.39	0	238.9	267.48	0	845.1	3	4.5	3	64.12	121.15	−3.14	−4.07	−5.18	53.75	−1.86
SANC00688	503.38	64.12	191.17	248.09	0	852.22	4	4.7	3	72.82	94.05	−2.9	−3.5	−4.92	152.41	−1.39
SANC00467	486.52	47.75	143.78	294.99	0	816.96	1	3.25	3	88.05	77.75	−3.68	−3.94	−5.06	428.96	−0.83

SASA=Solvent accessible surface area, FOSA=Hydrophobic component of SASA, FISA= Hydrophilic component of SASA, PISA = Pi (flat) component of SASA, WPSA = Total SASA excluding PISA, RO5/3 = Role of Five/Three, Volume = Molecular volume, DonorHB = Estimated number of hydrogen bonds donated by the molecule, AccptHB = Estimated number of hydrogen bonds accepted by the molecule, HOA = Predicted human oral absorption on 0–3 scale, PHO = Percentage of oral absorption, PSA = Polar surface area, QplogS = Predicted aqueous solubility, CIQPlogS = Consensus log S (average of two prediction methods), QPlogHERG = Predicted IC50 value for blockage of HERG K+ channels, QPPCaco = Predicted apparent Caco-2 cell permeability, QPlogBB = Predicted brain/blood partition coefficient.

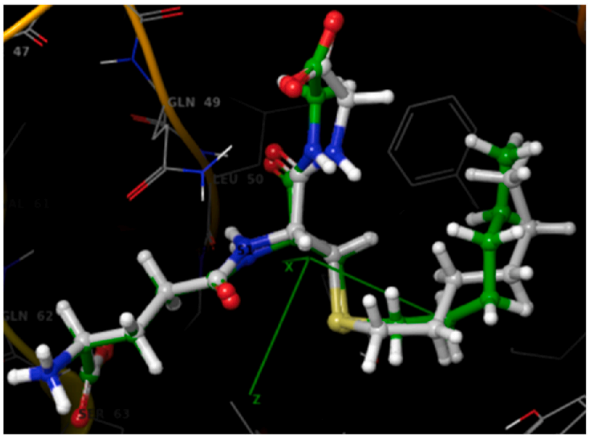

Fig. 2. Superimposition of co-crystallized (bleu) and docking (green) poses of the same ligands (RMSD = 1.235 Å). (For interpretation of the references to color in this figure legend, the reader is referred to the Web version of this article.)

2.3. Validation of docking protocol

The docking methodology was confirmed by calculating the root mean square deviation (RMSD) of docking the native ligand (co-crystal ligand, s-hexyl-GSH) with the prepared crystal structure of the primary protease of the receptor.

2.4. Molecular dynamics

The optimum docked complex, protein with ligand SANC00569, and SANC00689 were subjected for MD simulation study to validate the molecular docking based analysis and to study the protein-ligand dynamic behavior over a period of 200 ns, using Desmond software [17]. Considering the protein with 208 residues (3420 atoms), ligand with 44, 362.339 au, atoms, Atomic Mass, the system was neutralized by adding 23 Na^+ ions and 25 Cl^- ions, the total count of the system was 28580 atoms. The NPT ensemble with the temperature 300 K and a pressure 1 bar was applied in the run and the duration of simulation was 200 ns. The complex was solvated using SPC/TIP3P water body and OPLS4 force field parameters were used for MD simulations [18].

3. Results and discussion

This paper discusses the results of a virtual screening protocol followed by the molecular dynamics of the best ligand to select hit compounds for prospective experimental testing as inhibitors of the Onchoverca *volvulus* π-class glutathione *S*-transferase. Fig. 1 depicts an overview of the virtual screening protocol.

3.1. ADMET screening

To avoid unfavorable ADMET (Absorption, Distribution, Metabolism, Excretion, and Toxicity) properties, the pharmacokinetics and toxicity should be taken into account at the very first stage of drug development [19]. The potential druggability of the compounds were predicted using QikProp. In this study, we preliminarily computed the ADMET properties of the data base. Results of the 12 selected hit compounds are tabulated in Table 1.

From Table 1, it can be seen that ligands namely SANC00689, SANC00335, SANC00263, SANC00106, SANC00643, SANC00105, SANC00688, and SANC00467 show high PHO, HOA, and QPPCaco values suggesting good oral absorption and permeability. While, SANC00101, SANC00263, and SANC00106 present lower PSA and higher lipophilicity (QplogS) enabling them to better penetrate cells and distribute spread in tissues. SANC00569, SANC00101, SANC00689, and SANC00335 have exposed hydrophobic regions (high FOSA) and H-bonding groups (donorHB, acceptHB) which are susceptible to metabolic enzymes like cytochrome P450. SANC00520, SANC00317, and SANC00467 show low molecular weight and polarity (low PSA) which can favor excretion in urine. One way of ranking the ligands from the most to the least likely to be good drug candidates is based on the overall ADMET profiles. From these profiles, it can be admitted that: 1) SANC00689 has high cell permeability, solubility and oral absorption (PSA), low PSA and high lipophilicity enable good distribution, low risk of cardiotoxicity; 2) SANC00569 shows strong absorption and distribution properties, and slightly higher metabolism risk due to hydrophobic regions, and low brain penetration. To sum up, SANC00689 has the most optimal overall drug-like properties followed by SANC00569 and SANC00335. The top hits have the right balance of adsorption, distribution, metabolism and excretion potential.

Table 2
Docking scores and MMGBSA binding affinities of the selected hits.

No	Docking score (kcal/mol)	No. of H-bond/Pi-Pi Stacking	Interacting Amino acid residue	MMGBSA
s-hexyl-GSH	−8.03	07 H-bond 01 Salt Bridge	02Leu50, Gln49, 02Ser63, Gln62, Arg95 Lys42	−67.9
SANC00569	−8.34	04 H-bond 02 Pi-Pi Stacking	02 Leu50, Tyr7, Phe8 02 Phe8	−46.09
SANC00101	−7.39	03 H-bond 01 Pi-Pi Stacking	02 Leu50, Thr102 Phe8	−39.31
SANC00689	−6.36	03 H-bond 02 Pi-Pi Stacking	Lys32, Leu50, Typ7 Phe8, Phe38	−46.26
SANC00317	−5.73	02 H-bond	02 Leu50	−41.04
SANC00520	−5.65	02 H-bond 01 Pi-Pi Stacking	Leu50, Tyr7 Tyr7	−31.58
SANC00335	−5.63	05 H-bond 01 Pi-Pi Stacking	Lys35, Lys42,Gln49,Tyr7 Phe38	−41.23
SANC00263	−5.48	03 H-bond	Leu50, Gly204, Tyr7	−38.83
SANC00106	−5.32	02 H-bond	02 Leu50	−38.23
SANC00643	−5.31	03 H-bond 01 Pi-Pi Stacking	Leu50, Thr102 Phe8	−37.92
SANC00105	−5.31	02 H-bond	Leu50, Tyr7	−29.7
SANC00688	−5.15	03 H-bond	Leu50, Tyr7, Thr102	−43.87
SANC00467	−5.11	04 H-bond	Arg95, 02 Ser63, Gln49	−15.62

3.2. Docking

3.2.1. Docking validation

Before finding the potent *Onchoverca volvulus* pi-class glutathione *S*-transferase (Ov-GST2) inhibitors, the performance of Schrödinger software in predicting inhibitor-Ov-GST2 binding mode and affinity was first evaluated. The native bound s-hexyl-GSH ligand was removed and re-docked using the extra precision (XP) glide docking, and the binding mode was inspected (Fig. 2). A comparison of the re-docked structure with the native structure revealed that maestro's Schrödinger suites meticulously predicted the correct binding mode of Ov-GST2 with the active site constituted of Tyr7, Phe8, Ile10, Leu13, Phe38, Lys35, Lys42, Gly48, Gln49, Leu50, Pro51, Gln62, Ser63, Gly64, Arg95, and Tyr106 keys amino acids. Native ligand exhibited seven substantial H-bonds with Leu50, Gln49, 02Ser63, Gln62, and Arg95, and one salt bridge with Lys42.

Molecular docking provides a visible tool to predict the binding orientation of ligands to their protein targets, the docking score is widely used to evaluate the affinity and activity of the ligands. All compounds were docked to Ov-GST2. Detailed binding modes of the 12 selected compounds to Ov-GST2 were investigated and depicted in Table 2 and Fig. 3.

An analysis of Table 2 shows that docking score of the selected hits are ranged from −8.34 to −5.11 kcal mol^{-1}, while Fig. 3 shows that all these compounds (all the homoisoflavanones) are within the binding site, interacting with the key amino acid residues. Compound SANC00569 presents the highest affinity for the target, with a docking score of −8.34 kcal mol^{-1} lower by 0.31 kcal mol^{-1} compared to the native ligand. 00569 experiences four H-bonds interactions with Leu50, Tyr7 and Phe8 residues, two Pi-Pi stacking interaction with Phe8. Additionally, 00569 simulates non-bonded interactions (hydrophobic and polar), with Leu50, Pro51, Tyr7, Phe8, Ile10, Leu13, Tyr106 and Gln49 amino acids, nearly similar to the binding mode of the native ligand. The binding pose explained the potential affinity of compound SANC00569 confirming it as the most hypothetical lead inhibitor against Ov-GST2. In addition, the MMGBSA calculation reveals that SANC00569, and SANC00689 have the lowest binding energies of −46.09, and −46.26 kcal mol^{-1}, respectively. Overall, the docking score and MMGBSA results indicate that hits SANC00569, and SANC00689 have high affinity for the target and are well-suited for further optimization as antifilarial leads. The modeling predicts they bind strongly in the active site. To the best of our knowledge, there is no report of any alleged anti–onchocerciasis activity referring to homoisoflavanones or flavonoids. Nevertheless, homoisoflavanones, which are a subclass of flavonoids, exhibit a plethora of biological activities [20,21]. In 2007, C. Koorbanally et *al.* [21] found that homoisoflavanones with similar structure to compound SANC00569 and SANC00689 exhibited antimicrobial activity. Then compound SANC00569 named 3,5,6-trihydroxy-7-methoxy-3-(3′-hydroxy-4′-methoxybenz yl)-4-chromanone], and compound SANC00689 [5-hydroxy-3-4-hydroxybenzyl)-7-methoxy-4-chromone were selected for MD run of 200 ns.

3.3. Molecular dynamics simulation

Molecular dynamics simulation was further performed to investigate the stability of the_Ov-GST2_SANC00569 complex obtained by molecular docking. The complex was perturbed in water at a normal temperature (300 °C) and pressure (1.00 atm) for 200 ns run.

The structural changes of the Ov-GST2_SANC00569 complex were examined using root mean square deviation (RMSD). The conformational change of backbone atoms was estimated and compared to the initial conformation over 200 ns of MD simulations. As can be seen in Fig. 4, the overall stability of the investigated complex was observed with a protein's RMSD value (left Y-axis) ranging from 0.9 to 2.7 Å. Its fluctuations towards the end of the simulation are around some thermal average structure. From about 80 ns to the end of the simulation time, the RMSD values of the protein stabilize at around 2.4 Å, indicating that the simulation converges, then,

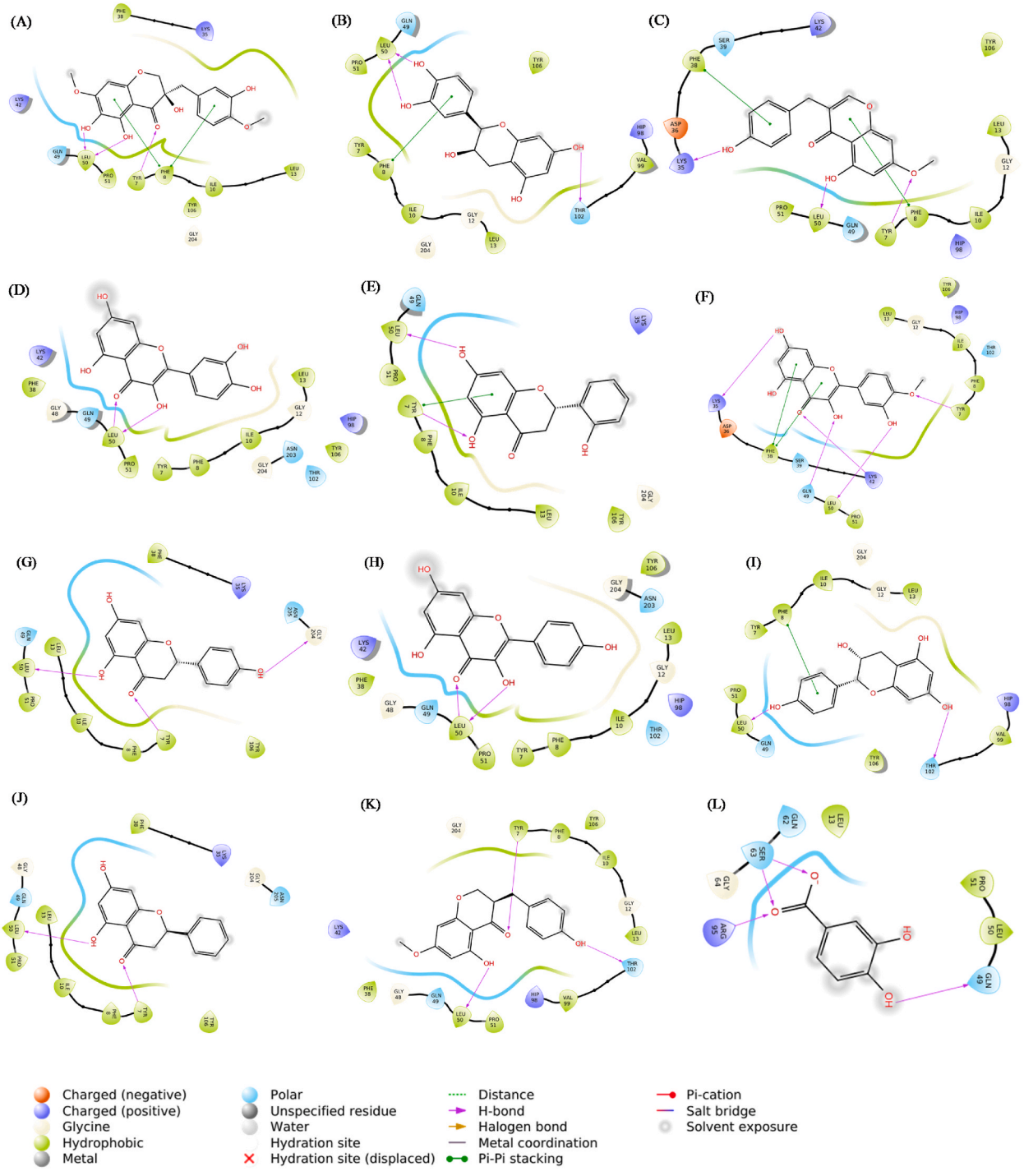

Fig. 3. Binding mode predictions for the 12 selected hits with O. *volvulus* pi-class glutathione *S*-transferase (PDB: 1tu8): (A)- SANC00569, (B)- SANC00101, (C)- SANC00689, (D)- SANC00317, (E)- SANC00520, (F)- SANC00335, (G)- SANC00263, (H)- SANC00106, (I)- SANC00643, (J)- SANC00105, (K)- SANC00688, (L)- SANC00467.

the system has reached an equilibrium state. Furthermore, ligand RMSD (right Y-axis) indicates how stable the ligand is with respect to the protein and its binding pocket. At the end of the simulation time, the RMSD value of the ligand is 7.226 Å, higher than that of protein by 4.891. Therefore, it is certain that the ligand has not diffused away from its initial binding site. Overall, these results confirmed that the 3,5,6-trihydroxy-7-methoxy-3-(3′-hydroxy-4′-methoxybenzyl)-4-chromanone inhibitor is tightly bonded and does not affect the overall topology of Ov-GST2.

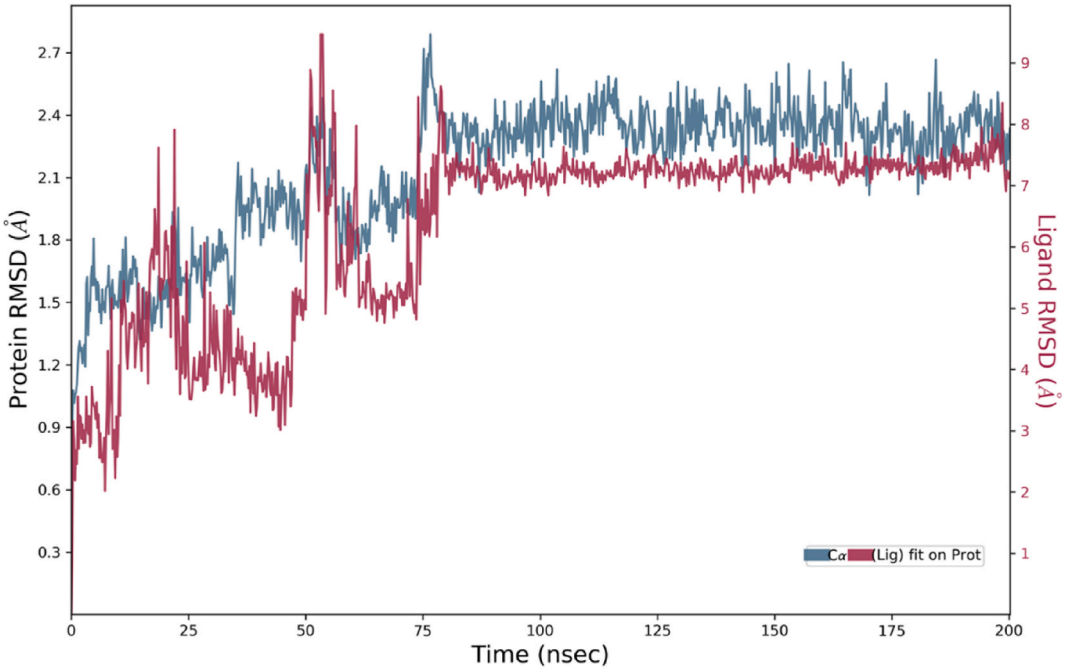

Fig. 4. Protein-ligand root mean square deviation (RMSD).

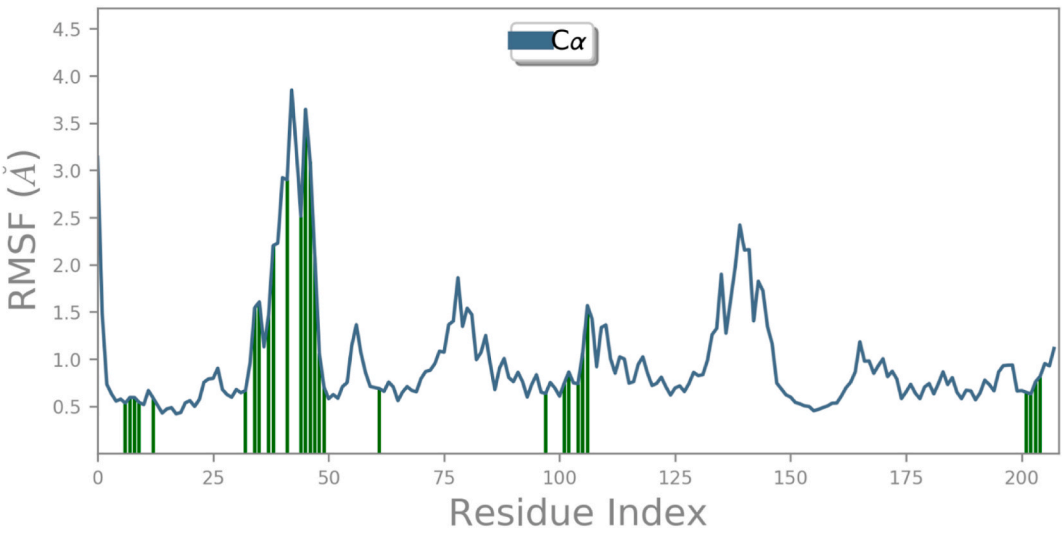

Fig. 5. Protein root mean square fluctuation (RMSF).

Moreover, the MMGBSA and its standard deviation for the last 20-ns [process frame 907–1002] have been performed, and the outcomes indicate that the free energy of the binding of SANC00569 to Ov-GST2 ranges from −57.0265 to −48.6293 kcal/mol, with an average value of −52.8279 kcal/mol and a standard deviation of 4.20. These results are in perfect agreement with the MMGBSA obtained after the docking calculation and the RMSD analysis.

To characterize local changes along the Cα protein backbone during simulation, the protein and ligand Root Mean Square Fluctuation (RMSF) have been performed and the results are shown in Figs. 5 and 6, respectively. In Fig. 5, peaks indicate areas of the protein that fluctuate the most during the simulation. And protein residues that interact with the ligand are marked with green-colored vertical bars. We observe that the N- and C-terminal fluctuate less than parts of the protein ranging from residue index 30 to index 49. These regions can be attributed to looped regions of the protein that are typically less stable. Heavy atoms were used to calculate ligand RMSF to give novel insight about how the molecule moves (Fig. 6). 3,5,6-trihydroxy-7-methoxy-3-(3′-hydroxy-4′-methoxybenzyl)-4-chromanone shows the greatest fluctuation at the sp^3 carbon bounding the phenyl and bicyclic groups with an average of 2.0 Å

Fig. 6. The ligand root mean square fluctuation (L-RMSF).

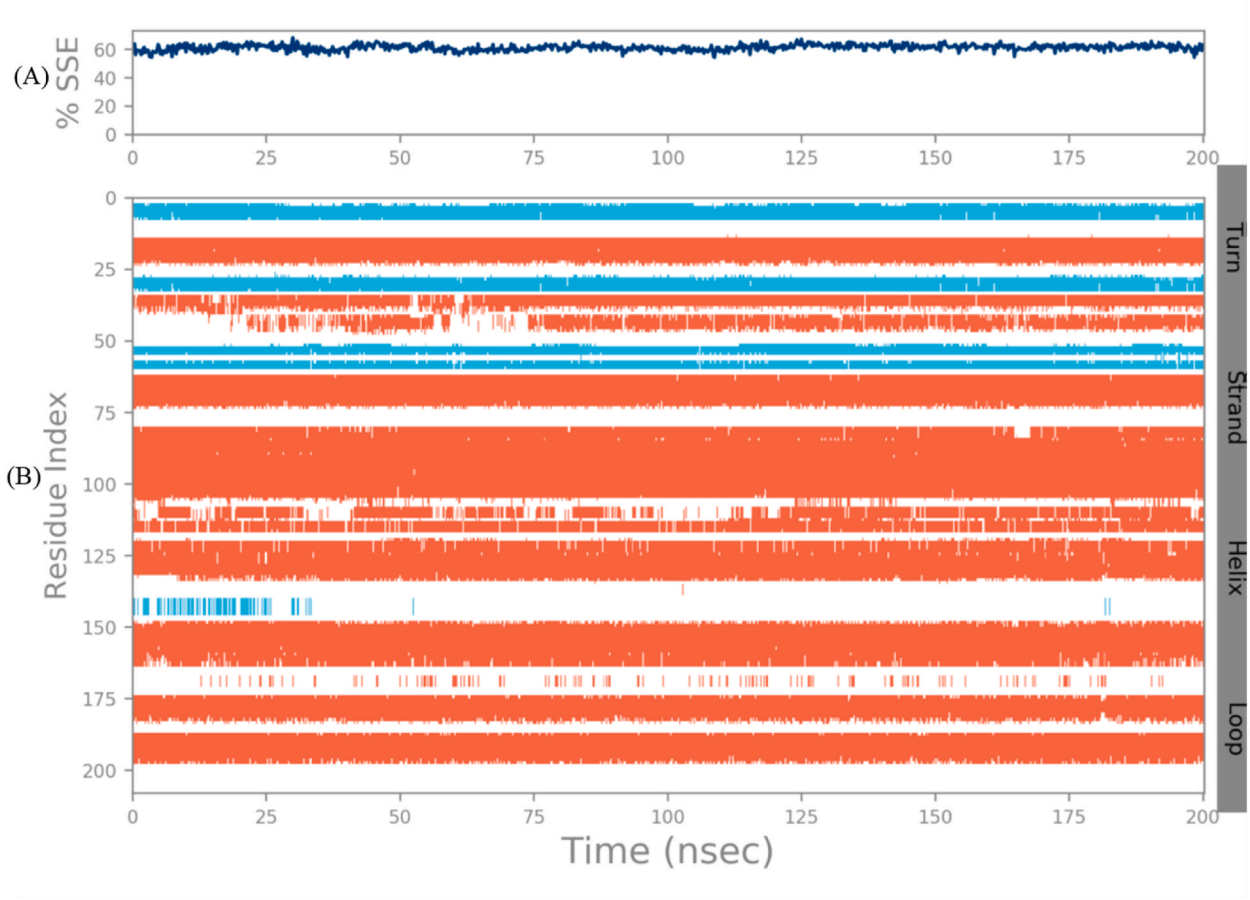

Fig. 7. (A)- Protein Secondary Structure composition for each trajectory frame over the course of the simulation, and (B)- SSE's residue assignment over time.

fluctuation.

Protein secondary structure elements (SSE) like alpha-helices and beta-strands are monitored throughout the simulation, and the results are depicted in Fig. 7. The plot below summarizes the SSE composition for each trajectory frame over the course of the simulation, and the plot at the bottom monitors each residue and its SSE assignment over time. The secondary structural organization of 3,5,6-trihydroxy-7-methoxy-3-(3′-hydroxy-4′-methoxybenzyl)-4-chromanone remained intact over the simulation time with a little decrease in the helical and strand content as can be seen in Fig. 7.

Contributions of H-bonds, hydrophobic, ionic interactions and water bridges were monitored over the course of simulation time. During the molecular dynamics, some of the interactions observed in the docking were lost, but new interactions were found to take place. For example, H-bond with Phe8 was lost, whereas H-bond with residues such as Lys35, Gly48, Gln49, and Tyr106 were observed, even though not very consistent. Two H-bond interactions were very prominent with Leu50, and Tyr7. Interactions with

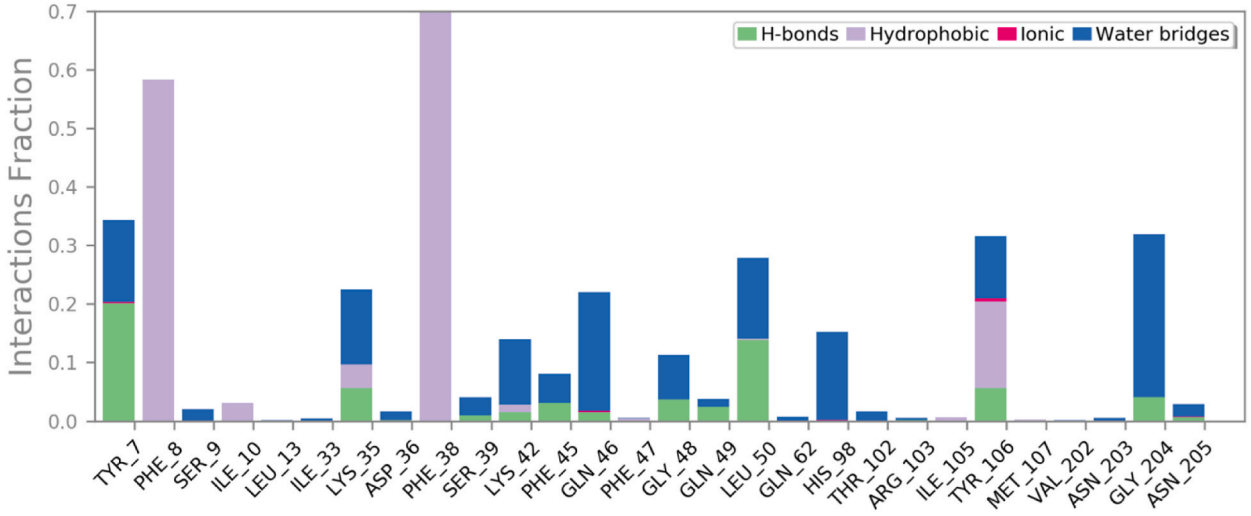

Fig. 8. Protein-ligand interactions (or 'contacts').

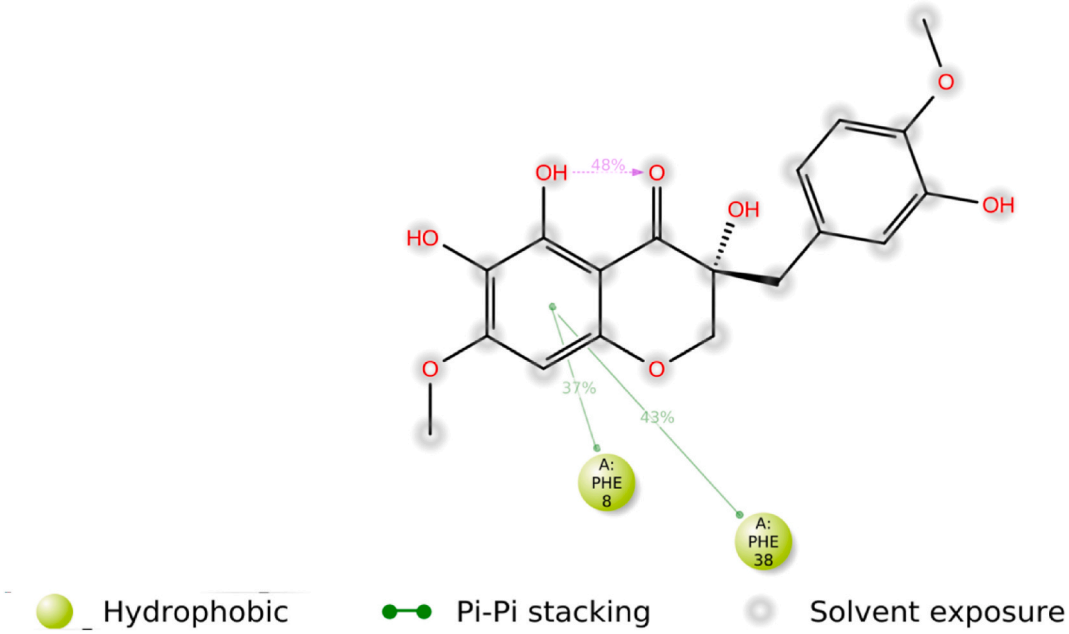

Fig. 9. Ligand atom interactions with the protein residues.

Phe8 and Phe38 were also observed, and it was mostly through hydrophobic contacts (Fig. 8). A schematic representation of detailed ligand atom interactions with the protein residues is depicted in Fig. 9. It can be seen that the hydrophobic interactions with Phe8 and Phe38 occur at 37.0 % and 43.0 % of the simulation time in the selected trajectory. These interactions are hypothetically observed on the most substituted aromatic ring where the π-delocalization should be high. It can also be observed that the intramolecular H-Bond occurs at 48.0 % of the simulation time, and involves the carbonyl group and the hydrogen atom of the hydroxyl group nearest to it in the aromatic ring.

Fig. 10 depicts the properties the ligands, such as the ligand RMSD with respect to the reference conformation (typically the first frame) (A), radius of gyration (rGyr) (B), Intramolecular H-Bonds (intraHB), Molecular Surface Area (MolSA), Solvent Accessible Surface Area (SASA), and Polar Surface Area (PSA), ranging from the top to the bottom, respectively. An analysis of Fig. 10 shows that the ligand RMSD, and rGyr, fluctuate at around 1.9 and 4.3 Å, respectively. The number of internal H-bonds (HB) within a ligand molecule oscillate between 0 and 1. Finally, Molecular Surface Area (MolSA), Solvent Accessible Surface Area (SASA), and Polar Surface Area (PSA) keep nearly the same values till the end of the simulation time, with average valuers of 315, 150 and 220 $Å^2$, respectively.

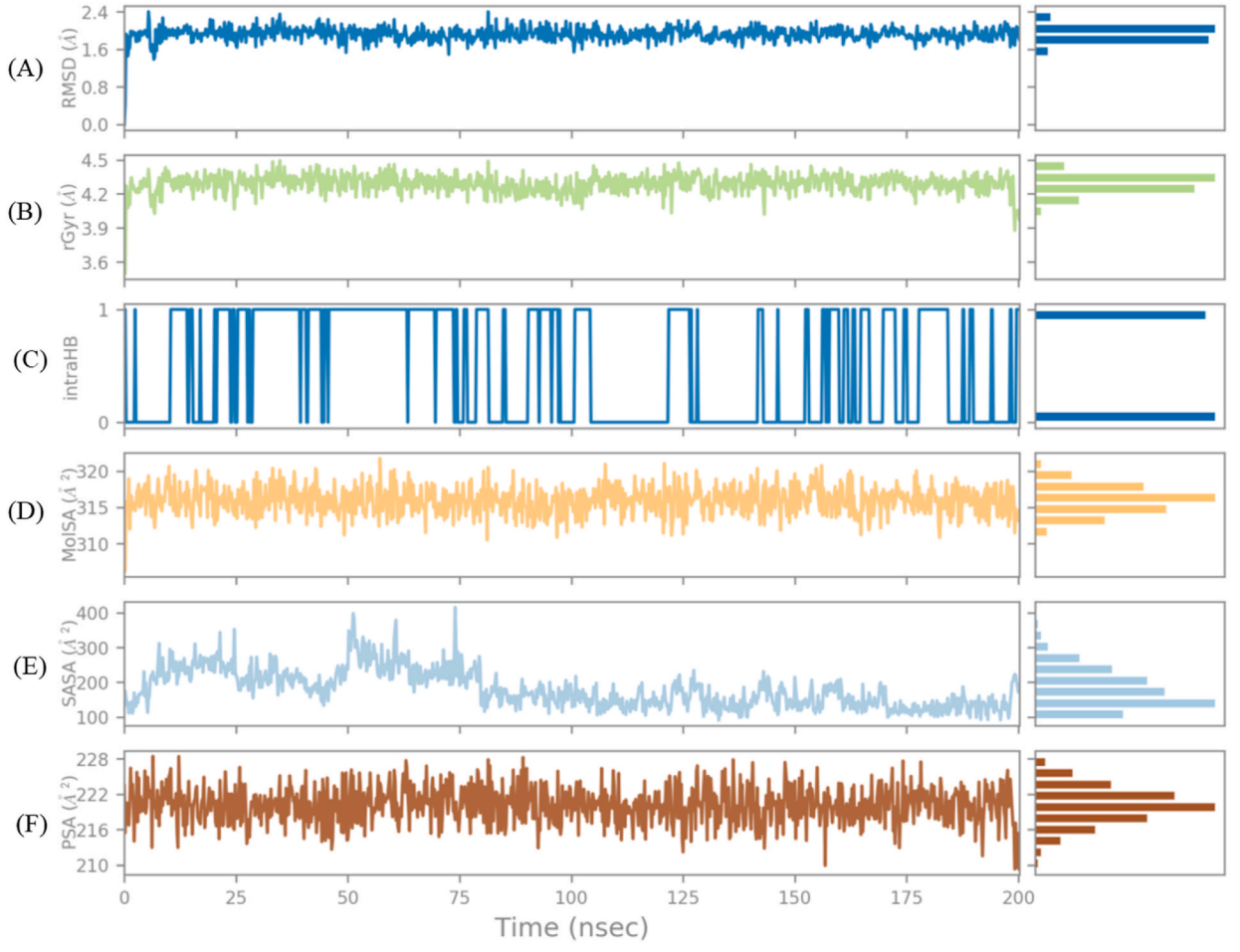

Fig. 10. Ligand Properties: (A)- RMSD with respect to the reference conformation (typically the first frame), (B)- radius of gyration (rGyr), (C)- Intramolecular H-Bonds (intraHB), (D)- Molecular Surface Area (MolSA), (E)- Solvent Accessible Surface Area (SASA), (F)- Polar Surface Area (PSA).

4. Conclusions

Herein, we report a virtual screening protocol of 1012 natural products from SANCBD, that were tested to identify potential drug candidates for the inhibition of the onchocerciasis. ADMET, results showed that compound SANC00689 has the most optimal overall drug-like properties followed by SANC00569 and SANC00335. Meanwhile, the docking and MMGBSA calculations reveal that SANC00569, and SANC00689 have the lowest binding energies mechanism of −46.09, and −46.26 kcal/mol, respectively. Molecular dynamics run of 200 ns showed that the SANC00569 inhibitor is tightly bonded and does not affect the overall topology of Ov-GST2. This protocol allowed the identification of the homoisoflavanones, named 3,5,6-trihydroxy-7-methoxy-3-(3′-hydroxy-4′-methoxybenzyl)-4-chromanone, as potential Ov-GST2 inhibitor. The Ov-GST2 inhibitor reported in the present work may serve as guide for further experimental studies on the aforementioned compound for its inhibit properties on *O. volvulus* pi-class glutathione *S*-transferase.

Ethics statement

All authors have been personally and actively involved in substantial work leading to the paper, and will take public responsibility for its content.

Data availability statement

The authors confirm that the data supporting the findings of this study are available within the article.

CRediT authorship contribution statement

Mbah Bake Maraf: Writing – review & editing, Writing – original draft, Visualization, Validation, Formal analysis, Data curation, Conceptualization. **Bel Youssouf G. Mountessou:** Writing – review & editing, Data curation. **Tsahnang Fofack Hans Merlin:** Writing – review & editing, Formal analysis, Data curation. **Pouyewo Ariane:** Investigation, Data curation. **Joëlle Nadia Nouping Fekoua:** Methodology, Investigation. **Takoua Bella Jean Yves:** Visualization, Investigation, Formal analysis. **Tchuifon Tchuifon Donald Raoul:** Visualization, Formal analysis. **Auguste Abouem A Zintchem:** Writing – review & editing, Visualization. **Gouet Bebga:** Supervision, Formal analysis. **Ndassa Ibrahim Mbouombouo:** Supervision, Project administration, Conceptualization. **Ponnadurai Ramasami:** Writing – review & editing, Conceptualization.

Declaration of competing interest

The authors declare that they have no known competing financial interests or personal relationships that could have appeared to influence the work reported in this paper.

Acknowledgements

The authors thank the Molecular Topology and Drug Design Research Unit, Department of Physical Chemistry, Pharmacy Faculty, University of Valencia, 46100 Valencia, Spain, for computational resources. M. B. Maraf and T. F. Hans-Merlin Acknowledge Prof. Haydar A. Mohammad-Salim from Faculty of Science, Department of Chemistry, University of Zakho, Duhok 42001, Iraq, and Prof. Jesus Vicente de Julián-Ortiz from Molecular Topology and Drug Design Research Unit, Department of Physical Chemistry, Pharmacy Faculty, University of Valencia, 46100 Valencia, Spain, for mentoring.

References

[1] L.E. Coffeng, W.A. Stolk, H.G. Zoure, J.L. Veerman, K.B. Agblewonu, M.E. Murdoch, M. Noma, G. Fobi, J.H. Richardus, D.A.P. Bundy, D. Habbema, S.J. de Vlas, U.V. Amazigo, African programme for onchocerciasis control 1995-2015: model-estimated health impact and cost, PLoS Neglected Trop. Dis. 7 (1) (2013) e2032, https://doi.org/10.1371/journal.pntd.0002032.

[2] J.L. Eng, R.K. Prichard, A comparison of genetic polymorphism in populations of Onchocerca volvulus from untreated- and ivermectin-treated patients, Mol. Biochem. Parasitol. 142 (2005) 193–202, https://doi.org/10.1016/j.molbiopara.

[3] A. Ngwewondo, I. Scandale, S. Specht, Onchocerciasis drug development: from preclinical models to humans, Parasitol. Res. 120 (12) (2021) 3939–3964, https://doi.org/10.1007/s00436-021-07307-4.

[4] F.A. Ugbe, G.A. Shallangwa, A. Uzairu, I. Abdulkadir, Theoretical modeling and design of some pyrazolopyrimidine derivatives as Wolbachia inhibitors, targeting lymphatic filariasis and onchocerciasis, Silico Pharmacol 10 (1) (2022) 8, https://doi.org/10.1007/s40203-022-00123-3.

[5] A.S. Cabrera, V.B. Garcıa, C.L. Ortega, X. Guo, J.C. Basurto, R.P.A. Mario, A computational analysis of the binding mode of closantel as inhibitor of the Onchocerca volvulus chitinase: insights on macrofilaricidal drug design, J. Comput. Aided Mol. Des. 25 (2011) 1107–1119, https://doi.org/10.1007/s10822-011-9489-y.

[6] Y. Wu, R. Adam, S.A. Williams, A.E. Bianco, Mol. Biochem. Parasitol. 75 (2) (1996) 207, https://doi.org/10.1016/0166-6851(95)02529-4.

[7] A. Athar, C. Udenigwe, The discovery and application of inhibitors of glutathione S-transferase as therapeutic agents -A review, Curr. Bioact. Compd. 4 (2008) 41–50, https://doi.org/10.2174/157340708784533384.

[8] J.A. Metuge, K.D. Nyongbela, J.A. Mbah, M. Samje, G. Fotso, S.B. Babiaka, F. Cho-Ngwa, Anti-Onchocerca activity and phytochemical analysis of an essential oil from Cyperus articulatus L, *BMC Complement*, Altern. Med. 14 (2014) 223, https://doi.org/10.1186/1472-6882-14-223.

[9] B. Oliver-Bever, Medicinal Plants in Tropical West Africa, Cambridge University Press, London, 1986, pp. 123–169, https://doi.org/10.2307/2806966.

[10] a) Protein Preparation Wizard, Epik, Schrödinger, LLC, New York, NY, 2021;
b) Impact, Schrödinger, LLC, New York, NY; Prime, Schrödinger, LLC, New York, NY, 2021;
c) G.M. Sastry, M. Adzhigirey, T. Day, R. Annabhimoju, W. Sherman, Protein and ligand preparation: parameters, protocols, and influence on virtual screening enrichments, J. Comput. Aided Mol. Des. 27 (3) (2013) 221–234, https://doi.org/10.1007/s10822-013-9644-8.

[11] E. Harder, W. Damm, J. Maple, C. Wu, M. Reboul, J.Y. Xiang, L. Wang, D. Lupyan, M.K. Dahlgren, J.L. Knight, J.W. Kaus, D.S. Cerutti, G. Krilov, W. L Jorgensen, R. Abel, R.A. Friesner, OPLS3: a force field providing broad coverage of drug-like small molecules and proteins, J. Chem. Theor. Comput. 12 (1) (2015) 281–296, https://doi.org/10.1021/acs.jctc.5b00864.

[12] Maestro, Schrödinger, LLC, New York, NY, 2021.

[13] LigPrep, Schrödinger, LLC, New York, NY, 2021.

[14] QikProp, Schrödinger, LLC, New York, NY, 2021.

[15] a) R.A. Friesner, R.B. Murphy, M.P. Repasky, L.L. Frye, J.R. Greenwood, T.A. Halgren, P.C. Sanschagrin, D.T. Mainz, Extra precision glide: docking and scoring incorporating a model of hydrophobic enclosure for protein-ligand complexes, J. Med. Chem. 49 (2006) 6177–6196, https://doi.org/10.1021/jm051256o;
b) T.A. Halgren, R.B. Murphy, R.A. Friesner, H.S. Beard, L.L. Frye, W.T. Pollard, J.L. Banks, Glide: a new approach for rapid, accurate docking and scoring. 2. Enrichment factors in database screening, J. Med. Chem. 47 (2004) 1750–1759, https://doi.org/10.1021/jm030644s;
c) R.A. Friesner, J.L. Banks, R.B. Murphy, T.A. Halgren, J.J. Klicic, D.T. Mainz, M.P. Repasky, E.H. Knoll, D.E. Shaw, M. Shelley, J.K. Perry, P. Francis, P. S. Shenkin, Glide: a new approach for rapid, accurate docking and scoring. 1. Method and assessment of docking accuracy, J. Med. Chem. 47 (2004) 1739–1749, https://doi.org/10.1021/jm0306430.

[16] J. Li, R. Abel, K. Zhu, Y. Cao, S. Zhao, R.A. Friesner, The VSGB 2.0 model: a next generation energy model for high resolution protein structure modeling, Proteins 79 (2011) 2794–2812.

[17] W.L. Jorgensen, D.S. Maxwell, J. Tirado-Rives, Development and testing of the OPLS all-atom force field on conformational energetics and properties of organic liquids, J. Am. Chem. Soc. 118 (1996) 11225–11236, https://doi.org/10.1021/ja9621760.

[18] G.A. Kaminski, R.A. Friesner, J. Tirado-Rives, W.L. Jorgensen, Evaluation and reparametrization of the OPLS-AA force field for proteins via comparison with accurate quantum chemical calculations on peptides, J. Phys. Chem. B 105 (2001) 6474–6487, https://doi.org/10.1021/jp003919d.

[19] D.K. Walker, The use of pharmacokinetic and pharmacodynamic data in the assessment of drug safety in early drug development, Br. J. Clin. Pharmacol. 58 (6) (2004) 601–608, https://doi.org/10.1111/j.1365-2125.2004.02194.x.

[20] S. Kwon, S. Lee, M. Heo, B. Lee, X. Fei, T.W. Corson, S.-Y. Seo, Total synthesis of naturally occurring 5,7,8-trioxygenated homoisoflavonoids, ACS Omega 5 (2020) 11043–11057, https://doi.org/10.1021/acsomega.0c00932.

[21] K. Du Toit, E.E. Elgorashi, S.F. Malan, D.A. Mulholland, S.E. Drewes, J. Van Staden, Antibacterial activity and QSAR of homoisoflavanones isolated from six Hyacinthaceae specie, South Afr. J. Bot. 73 (2007) 236–241, https://doi.org/10.1016/j.sajb.2007.01.002.